Deposition temperature of some PDC deposits from the 1982 eruption of El Chichon volcano (Chiapas, Mexico) inferred from rock-magnetic data

(Article begins on next page)

24 April 2024

Deposition temperature of some PDC deposits from the 1982 eruption of El Chichón volcano (Chiapas, Mexico) inferred from rock-magnetic data

Roberto Sulpizio [a,*], Elena Zanella [b], José Luis Macías [c]

[a] *CIRISIVU, c/o Dipartimento Geomineralogico, Università di Bari, Via Orabona 4, 70125, Bari, Italy*
[b] *Dipartimento di Scienze della Terra, Università di Torino, Via Valperga Caluso 35, 10125, Torino, Italy*
[c] *Instituto de Geofisica, Universidad Nacional Autónoma de México, Coyoacán 04510, México, D.F., Mexico*

ABSTRACT

Thermal remanent magnetization (TRM) analyses were carried out on lithic fragments from two different typologies of pyroclastic density current (PDC) deposits of the 1982 eruption of El Chichón volcano, in order to estimate their equilibrium temperature (T_{dep}) after deposition. The estimated T_{dep} range is 360–400 °C, which overlaps the direct measurements of temperature carried out four days after the eruption on the PDC deposits. This overlap demonstrates the reliability of the TRM method to estimate the T_{dep} of pyroclastic deposits and to approximate their depositional temperature. These results also constraint the time needed for reaching thermal equilibrium within four days for the studied PDC deposits, in agreement with predictions of theoretical models.

Sedimentological analysis demonstrates that different thickness of aggrading granular dominated pulses does not affect significantly the estimated T_{dep} for the two studied PDCs. The component analysis highlights how the entrapment of a significant amount of pre-heated lithic fragments from the dome and the conduit walls reduced the cooling of the pyroclastic mixture.

© 2008 Elsevier B.V. All rights reserved.

1. Introduction

Pyroclastic density currents (PDCs) are among the most complex and dangerous volcanic phenomena. They are moving mixtures of particles and gas that flow across the ground, and originate in different ways and from various sources, during explosive eruptions or gravity-driven collapse of domes (e.g. Cas and Wright, 1987; Carey, 1991; Druitt 1998; Freundt and Bursik 1998; Branney and Kokelaar, 2002; Burgissier and Berganz, 2002; Sulpizio and Dellino, 2008). They pose serious problems for both human health and infrastructure, in areas of tens of square kilometers around volcanoes (e.g. Lipman and Mullineaux, 1981; Baxter et al., 2005). PDCs have very hostile nature, and their real time observation is difficult. This reduces our capability to record important physical parameters from direct observation, and increases the importance to indirectly gain information from field and laboratory studies.

Of particular interest is the assessment of the deposition temperature of PDCs, because it has relevance for both PDC dynamics and volcanic hazard mitigation. The deposition temperature of PDC deposits is a function of the initial temperature of the pyroclastic mixture, the size and provenance of its constituents, the cooling during transport, and the sedimentation rate. Estimation of the temperature of deposition can be addressed by measuring the thermal remanent magnetization (TRM) of lithic fragments in pyroclastic deposits. The measured values represent the temperature of equilibrium between the lithic clasts and the bulk PDC deposit, which is a function of the initial temperature of the different components and of the rate of cooling of the deposited mass (e.g. McClelland and Druitt, 1989; Cioni et al., 2004). The TRM technique has been successfully applied in several cases around the world (e.g. Wright, 1978; Hoblitt and Kellogg, 1979; Kent et al., 1981; McClelland and Druitt, 1989; Downey and Tarling, 1991; Clement et al., 1993; Mandeville et al., 1994; Bardot, 2000; McClelland et al., 2004). Recently this technique was applied to lithic fragments and human artifacts (tiles and pottery) embedded in the PDC deposits of AD 79 and AD 472 eruptions of Somma-Vesuvius (Cioni et al., 2004; Gurioli et al. 2005; Zanella et al., 2007, in press).

This paper deals with the assessment of equilibrium temperature of some PDC deposits of the 1982 eruption of El Chichón volcano, and represents the first tentative to apply the TRM technique to pyroclastic deposits of Mexican volcanoes. PDCs were abundantly generated during the 1982 eruption, and they deposited various thickness of pyroclastic material over a wide area all around the volcano edifice and surrounding areas (Fig. 1; Carey and Sigurdsson, 1986; Scolamacchia and Macías, 2005). The paucity of accessible outcrops after more

* Corresponding author.
E-mail addresses: r.sulpizio@geomin.uniba.it (R. Sulpizio), elena.zanella@unito.it (E. Zanella), macias@geofisica.unam.mx (J.L. Macías).
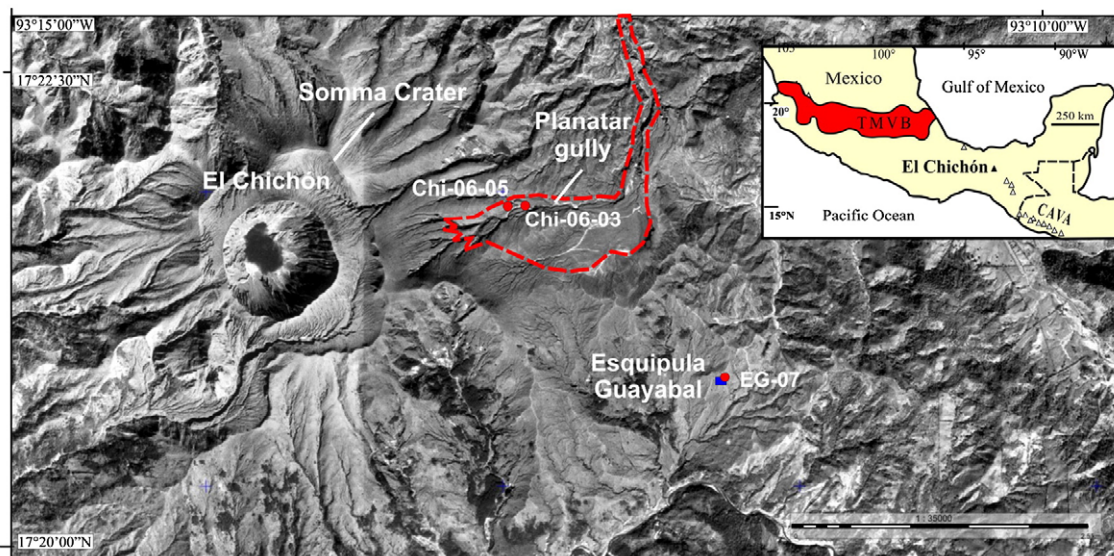
Fig. 1. Location map of sampling sites. The orthophoto was obtained from November 2000 air photographs scale 1:75,000 by Instituto Nacional de Estadística Geografía e Informática (INEGI). The spatial resolution of the image is 1.5 m. The red dashed line delimits the PF1 deposits along the El Platanar gully. PS1 deposits cover all the area shown in figure. Inset map shows the location of El Chichón volcano in southern México. Abbreviations are: TMVB = Trans-Mexican Volcanic Belt and CAVA = Central American Volcanic Arc. (For interpretation of the references to color in this figure legend, the reader is referred to the web version of this article.)

than 25 years of re-vegetation does not allow an extensive sampling throughout the eruptive succession, but the collected data yield important preliminary results.

2. The 1982 eruption

El Chichón is a late Pleistocene–Holocene volcano located in the State of Chiapas in southern Mexico. Prior to the 1982 eruption El Chichón consisted of a 2-km wide Somma crater, a central trachyandesitic dome and peripheral domes. In 1930, El Chichón volcano had an episode of seismic unrest accompanied by fumarolic activity that lasted a few months (Müllerried, 1933). Afterwards, El Chichón activity returned to background levels with the presence of weak fumaroles until 1980. New signs of volcanic unrest appeared in 1981, with increasing earthquakes, internal explosions, and fumarolic activity reported by geologists and local villagers (Canul and Rocha, 1981). The volcano reawakened in 1982, after 550 yr of quiescence

(Espíndola et al., 2000; Macías et al., 2003). The 1982 eruption began in March 28 with a 27 km high Plinian column that deposited fall layer A1 (Fig. 2; Carey and Sigurdsson, 1986) that opened a 300-m wide crater in the central dome (Medina-Martínez, 1982). Afterwards, the volcano remained relatively calm with variable but impending seismicity (Jiménez et al., 1999; Espíndola et al., 2000). Late on April 3, the most energetic event began (Yokoyama et al., 1992) with a series of hydromagmatic explosions that dispersed highly turbulent PDCs (PS1; Figs. 2 and 3a) around the volcano that killed more than 2000 people (Sigurdsson et al., 1984; Macías et al., 1997; Scolamacchia et al., 2005). These explosions opened the volcanic conduit and completely destroyed the central dome producing block-and-ash flows (PF1; Fig. 2) that filled valleys around the crater (Fig. 3b). Then, a series of small magmatic and hydromagmatic explosions emplaced PDCs (IU) in proximal areas followed by a 31-km high Phreatoplinian column that deposited fall layer B (Fig. 2). The column collapsed generating pumice-rich PDCs (PF2; Fig. 2) that further filled valleys around the
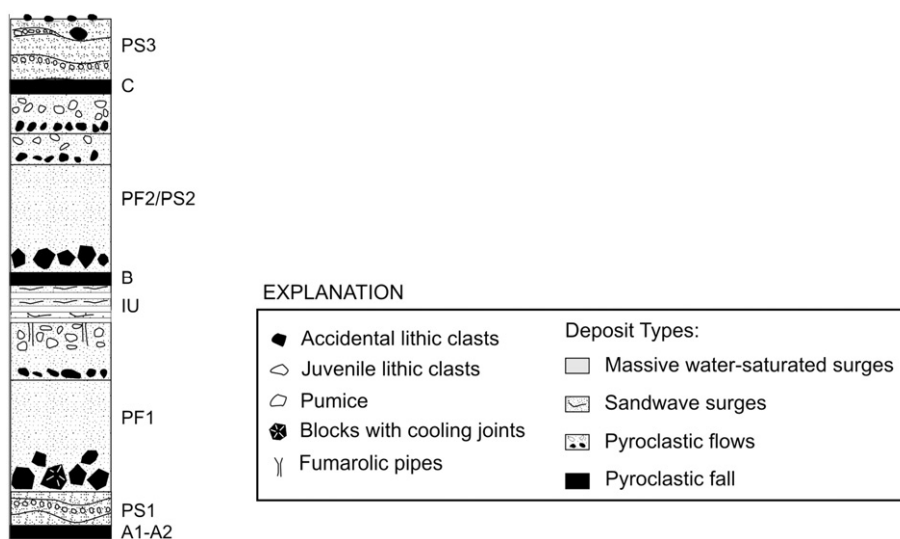
Fig. 2. Schematic stratigraphy of the 1982 eruption (Macías et al., 1997). Capital letters stand for: P = pyroclastic, F = flow, S = surge, IU = Intermediate Unit, and A, B, and C fall deposits.
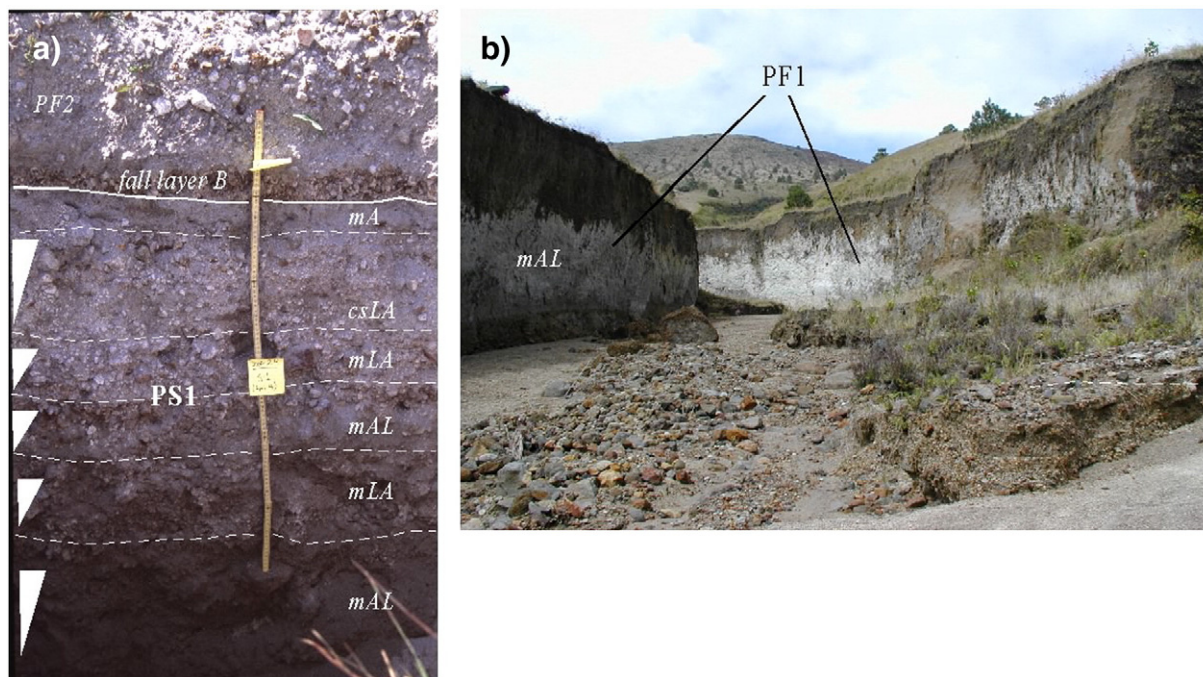
Fig. 3. a) View of PS1 deposits at Esquipula Guayabal site EG-07 in Fig. 1). In *italics* are indicated the lithofacies (see Table 1 for explanation). White dashed lines separate the different sub sub-depositional units. White triangles indicate repetitive inverse grading of deposits; b) View to the west of PF1 deposits. In the foreground is the deposit where samples were taken and El Chichón volcano in the background.

crater and reached distances of 8-km along the Platanar, Tuspac, and Agua Tibia valleys. This flow was followed by a diluted, turbulent PDC (PS2; Fig. 2) that was dispersed in all directions (Fig. 2). After 4 h the eruption restarted with another 29-km high Plinian column that deposited fall layer C. Afterwards, hydromagmatic explosions dispersed a diluted, turbulent PDC (PS3; Fig. 2) that traveled up to 3 km from the vent. Subsequent activity produced minor diluted PDCs localized inside the new 1-km wide crater reopened by the eruption. The eruption completely flattened ca. 100 km^2 of jungle with the emission of 1.1 km^3 of magma (Carey and Sigurdsson, 1986) of trachyandesitic composition that had a pre-eruptive temperature of 750–850 °C (Rye et al., 1984), 785±23 °C (Luhr et al., 1984), and 800 °C calculated experimentally (Luhr, 1990). A pumice flow deposit emplaced in April 4, extended to the outskirts of the Nicapa village 5-km NE (SEAN, 1989). In April 8, temperatures measured with a thermocouple at 40 cm depth averaged 360 °C, and were as high as 402 °C (SEAN, 1989).

3. Analytical methods and results

3.1. Lithofacies analysis

Lithofacies analysis was carried out on PF1 and PS1 deposits at localities of sampling, located east of the volcano along the El Platanar valley and at Esquipula Guayabal village (Fig. 1). Stacked, generally inversely graded, decimeter-thick depositional sub-units, form the PS1 deposit at Esquipula Guayabal site (Fig. 3a; Table 1). No fine ash deposits nor erosions or volcaniclastic deposits are found interbedded in the PS1 stratigraphic succession indicating a rapid deposition of the different sub-units as concluded by several authors (Sigurdsson et al., 1984, 1987; Macías et al., 1997; Scolamacchia and Macías, 2005). Therefore, the repetitive occurrence of these massive to crudely stratified sub-units indicate deposition from decimeter-thick granular dominated flow-boundary zone (Branney and Kokelaar, 2002; Sulpizio et al., 2007) developed in a pulsating PDC (Sulpizio et al., 2007; Sulpizio and Dellino, in press). Sampled PF1 deposits at El

Platanar gully are massive, inversely graded, meter-thick ash and lapilli, and comprise at least two sub-depositional units (bottom and top in Fig. 2). Also in this case lithofacies analysis indicates deposition from a granular dominated flow-boundary zone developed within a pulsating PDC as attested by stratigraphic observations (Macías et al., 1997, 1998). During emplacement the moving flow (PF1) was channeled in the El Platanar gully, promoting thickening of the basal underflow up to some meters.

Table 1
Lithofacies codes and interpretation for PS1 and PF1 PDC deposits of Fig. 3

Lithofacies code	Description	Interpretation
mAL/mLA	Massive ash and lapilli. No sedimentary structures are visible, with the exception of a general reverse grading. Lithofacies mAL contains more ash than lapilli. The inverse for lithofacies mLA.	Deposition from a granular dominated flow flow-boundary zone, in which processes of kinetic sieving and kinematic squeezing promoted the concentration of large clasts at the top of the pulse that stopped abruptly (en masse freezing).
mA	Massive ash. No sedimentary structures. Ash with constant thickness at the scale of the outcrop.	Settling from the dilute ash cloud that accompanied the emplacement of the dense underflow whose deposits are described by lithofacies mAL/mLA and csLA. The absence of any sedimentary structure indicates very reduced lateral transport of particles.
csLA	Crudely stratified lapilli and ash. A faint stratification is visible, and mainly due to alignments of lithic lapilli. General reverse grading.	Deposition from a granular dominated flow flow-boundary zone, in which processes of kinetic sieving and kinematic squeezing promoted the concentration of large clasts at the top of the pulse. The faint, crude stratification indicates that traction processes played a limited role during deposition.
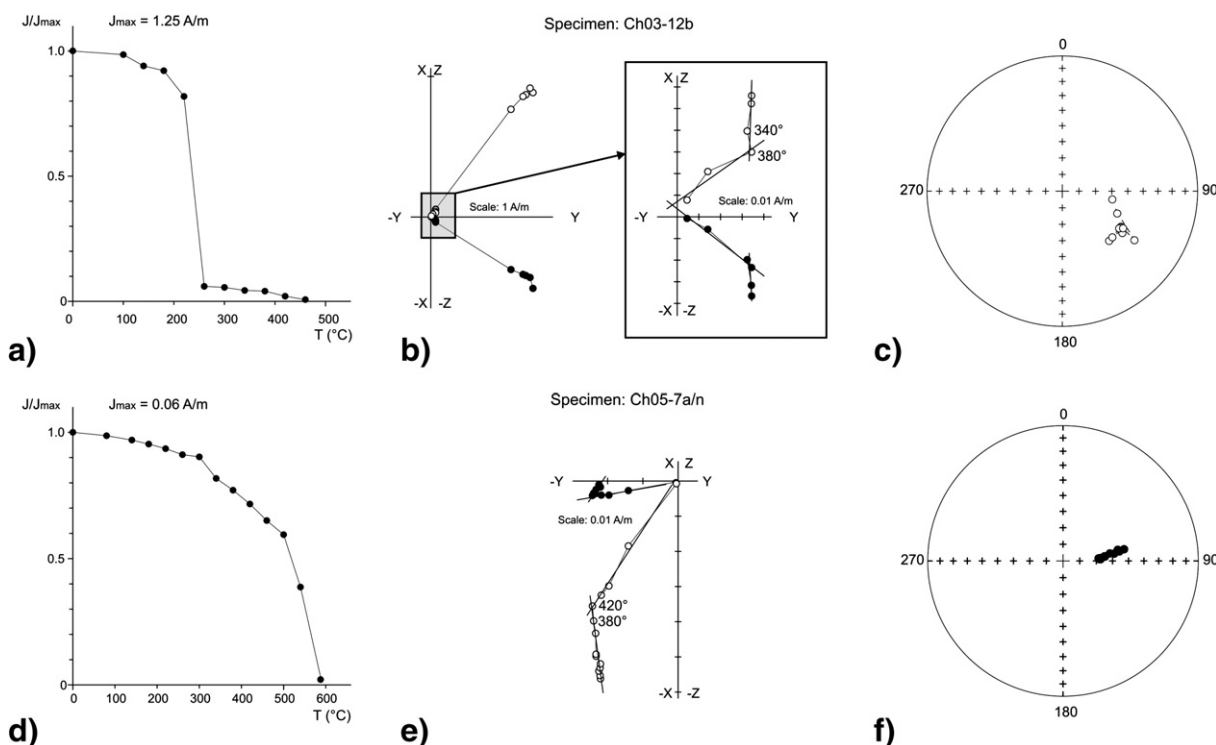
Fig. 4. Thermal demagnetization of lithic fragments from PF1 deposits of El Chichón. In a), d) normalized intensity decay curve; b), e) Zijderveld diagram. Symbol: full/open dot = magnetic declination/apparent inclination; figure = T value (°C); c), f) equiareal projection (full/open dot = positive/negative inclination). Directions in the Zijderveld diagrams are represented in the specimen reference system.

3.2. Component analysis and TRM data

Sampling of the lithic clasts embedded within the deposits was carried out on two PDC units of the stratigraphic succession (PS1 and PF1; Fig. 2). The samples were collected from unit PF1 at two localities along the El Platanar valley (Chi-06-03 and Chi-03-05; Fig. 1), and from unit PS1 at the remains of the Esquipula Guayabal village (EG-07; Fig. 1). Component analyses carried out in the −2, −1, and 0 ϕ fractions (4, 2 and 1 mm) of the PF1 deposits indicate that lithics are in average 27% by volume of the deposit, of which 12% are lithics from the dome, and 15% altered accidental lithics. Components analysis in the same fractions for PS1 (PS1-3 dry surge deposit) are in average 20% of the deposit, of which up to 6% are lithics from the dome, and up to 14% are altered accidental lithics. Assuming that these values represent the average content of lithic fragments for the whole PF1 and PS1 deposits, follows that around 50% and 30% of the lithic fragments of PF1 and PS1 deposits are from the pre-existing dome.

At least 10 lithic fragments (lava clasts), ranging in volume from 2 to 100 cm³, were selected at each site for TRM analyses, for a total of more than 40 samples. In two sites (Ch06-03 and Ch06-05) the size of the lava clasts was large enough to allow an accurate orientation of the samples. In these cases standard cylindrical specimens (ϕ=25.4 mm, h=22.5 mm) were subsequently cut in laboratory. Small, not oriented bits were sampled at sites Chi-06-05 and EG-07, and prepared for measurements using the plastic box plus Plasticine technique (Cioni et al., 2004).

To estimate the equilibrium temperature of the PDC deposits (T_{dep}), the lithic fragments were thermally demagnetized, following the procedure described in detail by Cioni et al. (2004) and Zanella et al. (2007a). It consists of stepwise heating/cooling cycles at progressive increasing temperatures. Steps of heating were fixed every 40 °C up to about 580 °C. After each step, remanent magnetization is measured and magnetic susceptibility is checked, to monitor possible mineralogical alteration induced by heating. Estimation of T_{dep} was achieved in 68 specimens (large samples were cut in

half and both parts were analyzed) at the ALP laboratory (Peveragno, Italy) using a JR-5 spinner magnetometer, a Schonstedt thermal demagnetizer and an AGICO KLY-3 bridge. Data have been interpreted with the principal component analysis (Kirschvink, 1980) and analyzed by using the Paleomac program (Cogné, 2003).

The TRM of a lava clast embedded in PDC deposits is typically characterized by two components: a high-temperature, primary component acquired during cooling of the volcanic rock from which the clast derives, and a low-temperature, secondary component acquired after reheating caused by transportation within the hot pyroclastic mixture and during cooling after deposition. The two remanence components are carried by grains with different blocking temperatures T_b (Butler, 1992), and the goal of stepwise demagnetization is to derive their T_b spectra. The temperature value which separates the two spectra is the reheating temperature and corresponds to T_{dep}. This value is clearly shown in the Zijderveld diagrams (Fig. 4b–e).

The lava clasts sampled at El Chichón group into two main classes, characterized by the different stability of the remanence with respect to temperature. The normalized intensity decay curves show that in the first class, around 90% of the initial natural remanent magnetization (NRM) is removed after heating to a peak temperature of about 240 °C (Fig 4a). In the second class, the intensity decay is slower and more than 50% of the initial NRM survives heating at 500 °C (Fig. 4d). In both classes no remanence is left at temperatures higher than 570–600 °C. This fact points to Ti-magnetite as the main ferromagnetic mineral and the different magnetic properties of the two classes may be tentatively ascribed to different sizes and/or Ti contents of the grains.

On the basis of the demagnetization pattern, Cioni et al. (2004) distinguished four Types (A to D) of thermal behaviors of clasts embedded in PDC deposits. More than 90% of the clasts collected from El Chichón deposit belong to types C and D, where the two components are respectively characterized by clearly isolated or partially overlapping T_b spectra, and the temperature range, including the actual reheating temperature, can be derived. Only five clasts do not provide temperature information; according to the classification

of Cioni et al. (2004), three are type A (minimum T_b higher than T_{dep}: no reheating overprint), and two are Type B (maximum T_b lower than T_{dep}: primary magnetization component fully erased).
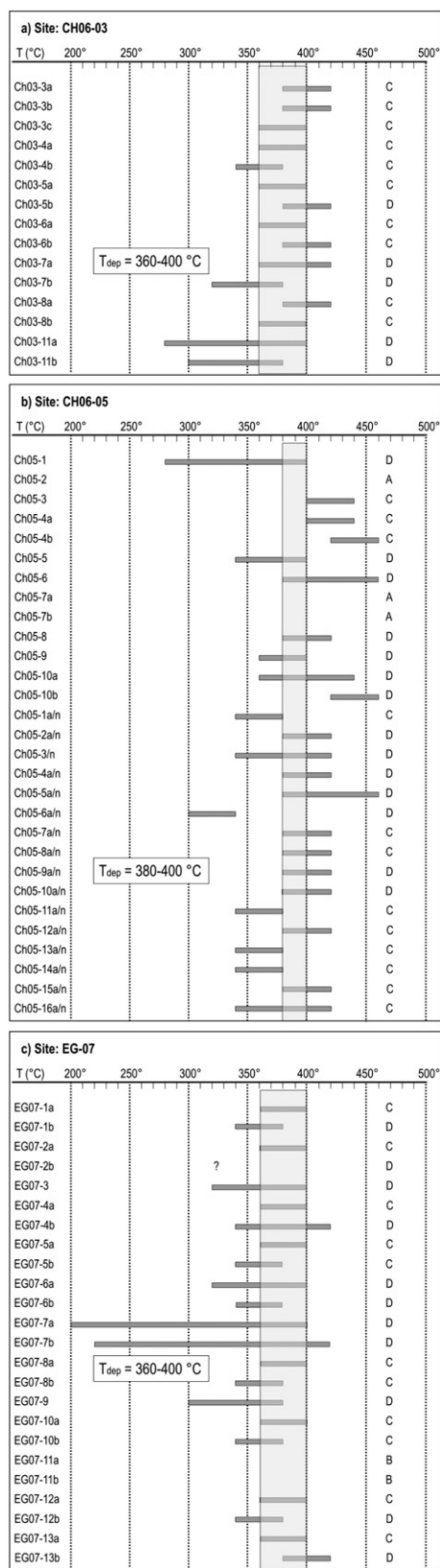

Fig. 5. Evaluation of T_{dep} of El Chichón PDC deposits by overlap of individual clasts reheating temperature ranges. For each specimen the thermal behavior type (A to D) is listed.

The examples shown in Fig. 4 are of Type C, in which the Zijderveld diagrams (Fig. 4b and e) are characterized by a knee-pattern that allows a clear-cut evaluation of the reheating temperature. In Fig. 4b, the low-temperature component is very well defined up to 380 °C (maximum angular deviation, MAD<2°) and the high-temperature component is defined between 380 and 460 °C, where only a mimimal minimal fraction of the initial NRM is left. The reheating temperature of the specimen falls therefore in the range 340 to 380 °C. A similar knee-pattern is also evident in Fig. 4e, where the reheating temperatures falls in the range 380 to 420 °C.

For each site, evaluation of T_{dep} was performed by the determination of the minimum temperature range in which the overlapping of individual clast reheating temperature ranges is maximum, as illustrated in Fig. 5 (Cioni et al., 2004). When possible, two specimens were measured from the same individual fragment to improve accuracy in the estimation (Fig. 5). Measured T_{dep} varies in the range 360–400 °C.

4. Discussion

4.1. What concurs to the temperature of a PDC?

PDC are flowing mixtures that comprise fluid (magmatic gases, air, water) and solid phases (juvenile, crystals and lithic fragments). The different phases concur differently to the average temperature of the PDC, and can be divided in heat-carrier (magmatic gases, crystals and juvenile fragments) and heat-absorber (lithic fragments). The temperature of the magma involved in the eruption defines the initial temperature of heat heat-carriers, which can be considered in thermal equilibrium when injected in the atmosphere (Dobran and Papale, 1993). Lithic fragments can be entrained in the eruptive mixture at different times, from the magma chamber walls, along the conduit due to erosion of wall rocks, at vent during crater erosion, or during motion of the PDC on volcano slopes. The temperature of the entrapped lithic fragments varies greatly in function of their source location, which can be close to the magmatic one for lithic fragments from the conduit walls and the dome, or close to the ambient temperature for those entrapped at vent or during PDC motion. Therefore, the amount of cool lithic fragments entrapped in the flowing mixture is crucial in determining the temperature of the PDC at any time and also the final equilibrium temperature (Marti et al., 1991). Component analysis showed that between 30% and 50% of the total lithics are from the pre-eruption dome. These dome-derived lithic fragments were incorporated in the pyroclastic mixture at higher temperature than the similar fragments from the volcano slopes, and can be considered at some extent as heat-carriers better than heat-absorbers. The same behavior can be assumed for lithic fragments eroded from the magma chamber and conduit walls, which add some other percentage to the amount of hot material entrapped in the PDCs. Therefore, the amount of cool lithic fragments is reduced at a few tens percentage of the whole PDC deposit, and this is reflected in the heat flow processes that determine the achievement of thermal equilibrium in the PDC mass. In particular, the low content of heat heat-absorber fragments with respect to the heat heat-carrier ones implies a higher amount of thermal energy available for their heating than in the case in which only cold lithic fragments are entrapped in the pyroclastic mixture, and this could reflect in a higher T_{dep} recorded by TRM.

Based on these considerations, the amount of lithic fragments seems not to have played an important role in substantially cooling the pyroclastic mixtures of PF1 and PS1 PDCs, and this suggests that the measured T_{dep} are very close to the real deposition temperatures.

4.2. Influence of sedimentary processes on T_{dep}

It has been argued that transport mechanisms and sedimentation/deposition processes can influence the emplacement temperature of

PDCs (Cioni et al., 2004). Although in principle correct, the effect of sedimentary processes on emplacement temperature is actually appreciable only when fluid turbulence is greatly enhanced by surface roughness (Gurioli et al., 2005; Zanella et al., 2007, in press). Lithofacies analysis of PF1 and PS1 deposits demonstrates they were emplaced under similar flow-boundary conditions, in which turbulence was inhibited by high particle concentration in the lower flow boundary. However, significant differences in the physical conditions at the time of deposition arise, if we consider the hypothesized thickness of the aggrading pulses that piled up to form PF1 and PS1 deposits. These were decimeter-thick granular flow-dominated pulses in the case of PS1 (Fig. 3a), and metric aggrading pulses in the case of PF1 (Fig. 3b). Since each aggrading pulse can be considered as a flow flow-boundary zone (Sulpizio et al., 2007; Sulpizio and Dellino, 2008), it can be argued that differences in their thicknesses could influence to reach the T_{dep} measured TRM values. Nevertheless, the PS1 and PF1 data demonstrate the reduced influence of thickness variation in granular flow-dominated flow flow-boundary zones, in which turbulence had a minor role or was absent during deposition.

4.3. Attainment of thermal equilibrium in PDCs

During the short time of motion of a small- to medium-scale PDC the temperature within the flowing mixture is not homogeneous, since it results from averaging the temperatures of its different components (lithics and juvenile fragments, magmatic gases and external fluids such as air and water; e.g. McClelland and Druitt, 1989; Cioni et al., 2004). This is because the different components are incorporated in the moving flow at different times and temperatures. The attainment of thermal equilibrium among the different components of the PDC involves heat flow from hot to cool components, and obeys the Fourier's law:

$$dQ/dt = -kA dT/dx \qquad (1)$$

where dQ/dt is the time rate of heat transfer, A is the area of the body the heat is to be transferred, dT/dx the temperature gradient and k the thermal conductivity coefficient of the material. The k coefficient is a material parameter, which depends on temperature and pressure range, density, porosity, fluid content and other physical parameters of the body (e.g. Dermici et al., 2004). The K value has a profound effect on time needed to reach thermal equilibrium among different materials.

However, when dealing with heat transfer, it is necessary to consider other thermo-physical properties of matter than the thermal conductivity k. These are the thermodynamic properties, which pertain to the equilibrium state of a system. Density (ρ) and specific heat (C_p) are two such properties used extensively in thermodynamic analysis. The product ρC_p, commonly termed the volumetric heat capacity, measures the ability of a material to store thermal energy (Özkahraman et al., 2004). Because substances with large density are typically characterised characterized by small specific heats, many solids and liquids have comparable heat capacities and are very good energy storage media ($\rho C_p > 1$ MJ/m³ K). Many rocks are also very good energy storage media, in this aspect. In turn, because of their very low density, gases are poorly suited for thermal energy storage ($\rho C_p \approx 1$ kJ/m³ K; Özkahraman et al., 2004).

In heat transfer analysis, the ratio of the thermal conductivity to the heat capacity is an important property termed the thermal diffusivity (α), which has units of m²/s:

$$\alpha = k/(\rho C_p). \qquad (2)$$

It measures the ability of a material to conduct thermal energy relative to its ability to store it. Materials with large α will respond quickly to changes in their thermal environment, while materials with small α will respond more sluggishly, taking longer to reach a new equilibrium condition.

The thermal diffusivity of common magmatic rocks is in the range of 10^{-6} m²/s (e.g. Vosteen and Schellschmidt, 2003), although up to one order of magnitude variations are possible as a function of porosity, density and temperature of the lithic fragment (Velinov et al., 1993). This range of diffusivity is comparable to that of liquid water (James, 1968), and at least two orders of magnitude less than that of dry air at 400–500 K. This means that lava fragments entrapped in the flow at ambient temperature significantly increase their temperature in a time that is usually longer than flow duration (Cioni et al., 2004). This implies that the most significant amount of heat flow going from hot material to the cooler fragments occurs within the deposit. Therefore it is important to consider the rate of heat lost from the bulk deposit to the surrounding environment. For a sub-aerial deposit the heat is exchanged mainly with the atmosphere and bedrocks, and temperature is strongly controlled by the thermal conductivity of the pyroclastic deposit as a whole. A key parameter for controlling the rate of heat loss in a porous material such a PDC deposit is its bulk density (solid mass/total volume), which strongly depends on the percentage of pores in the solid. Low bulk density implies a well developed network of voids filled by a light fluid (e.g. air), that drastically reduces the thermal conductivity of the deposit due to the low thermal conductivity of gas. The effective thermal conductivity of the pyroclastic deposit accounts for conduction through the solid materials, conduction or convection through the air in the void spaces, and, if the temperature is sufficiently high, radiation exchange between the surfaces of the solid matrix (e.g. Özkahraman et al., 2004). It is a matter of fact that lithified pyroclastic rocks (tuffs) are used in buildings as insulating material testifying their low heat conductivity.

Temperature decay patterns for small-sized PDCs are available in literature (e.g. Kozu, 1934; Ryan et al., 1990), which indicate these deposits are able to maintain internal temperatures between 300 and 400 °C for several days (Cioni et al., 2004). A thermal survey performed on small-volume hot debris avalanche deposits occurred at Stromboli volcano on December 29th, 2002, demonstrated that it maintained its internal temperature between 200 and 300 °C for more than three months, irrespectively of the rapid cooling of the external part that passed from 350–400 °C to less than 100 °C in about 25 days (Calvari et al., 2005).

Direct measurements carried out four days after the eruption on PDC deposits of El Chichón ($T=360–402$ °C; SEAN, 1989) overlap the T_{dep} assessed with the TRM method (360–400 °C; Fig. 5). This suggests that thermal equilibrium was attained by the analysed lava fragments within this time span, in agreement with previous calculations on PDC from other eruptions (e.g. PDC deposits of AD 79 eruption at Somma-Vesuvius; Cioni et al., 2004). These results demonstrate that TRM studies of lithic clasts constitute a reliable method for estimating not only the equilibrium temperature, but also the emplacement temperature.

5. Conclusions

The analysis of TRM of lithic fragments from PF1 and PS1 deposits of the 1982 eruption of El Chichón volcano highlights similar and overlapping T_{dep} in spite of their differences in depositional behavior. Component analysis of these deposits suggests the entrapment in the pyroclastic mixture of a significant amount of pre-heated lithic fragments from the dome and conduit walls as reflected in higher T_{dep} measured by TRM analysis. Measured T_{dep} overlap with direct measurements carried out four days after the eruption on PDC deposits, demonstrating the reliability of the method to assess equilibrium temperature within pyroclastic mixtures. How the T_{dep} is close to the depositional temperature depends on the cooling history of the pyroclastic deposit and on the amount of thermal energy loss by heating cool fragments and ingested air. However, the T_{dep} represents a lower constraint for the real depositional

temperature, which, in the case of the studied PDCs, was not less than 360–400 °C, a temperature able to immediately kill any human being along flow path, to burn trees and vegetation and to trigger fires over wide areas.

Acknowledgements

References

Bardot, L., 2000. Emplacement temperature determinations of proximal pyroclastic deposits on Santorini, Greece, and their implications. Bull. Volcanol 61, 450–467.

Baxter, P., Boyd, R., Cole, P., Neri, A., Spence, R., Zuccaro, G., 2005. The impacts of pyroclastic surges on buildings at the eruption of the Soufriere Hills volcano, Montserrat. Bull. Volcanol. 67, 292–313.

Branney, M.J., Kokelaar, P., 2002. Pyroclastic Density Currents and the Sedimentation of Ignimbrites. . Geological Society, 27. Memoirs, London. 143 pp.

Burgissier, A., Bergantz, G.W., 2002. Reconciling pyroclastic flow and surge: the multiphase physics of pyroclastic density currents. Earth Plan. Sc. Lett 202, 405–418.

Butler, R.F., 1992. Paleomagnetism. Blackwell Sci., Malden, Mass. 319 pp.

Calvari, S., Spampinato, L., Lodato, L., Harris, A.J.L., Patrick, M.R., Dehn, J., Burton, M.R., Andronico, D., 2005. Chronology and complex volcanic processes during the 2002–2003 flank eruption at Stromboli volcano (Italy) reconstructed from direct observations and surveys with a handheld thermal camera. J. Geophys. Res. 110, B02201. doi:10.1029/2004JB003129.

Canul, R.F., Rocha, V.L., 1981. Informe Geológico de la zona geotérmica de "El Chichonal", Chiapas. Internal Report, Comisión Federal de Electricidad, Morelia. 38 pp.

Carey, S.N., 1991. Transport and deposition of tephra by pyroclastic flows and surges. In: Fisher, R.V., Smith, G.A. (Eds.), Sedimentation in Volcanic Settings. SEPM, Special Publications, vol. 45, pp. 39–57.

Carey, S.N., Sigurdsson, H., 1986. The 1982 eruptions of El Chichón volcano, Mexico: 2. Observations and numerical modeling of tephra fall distribution. Bull. Volcanol 48, 127–141.

Cas, R., Wright, J.W., 1987. Volcanic Successions: Modern and Ancient. Allen and Unwin, London. 528 pp.

Cioni, R., Gurioli, L., Lanza, R., Zanella, E., 2004. Temperatures of the A.D. 79 pyroclastic density currents deposits (Vesuvius, Italy). J. Geophys. Res. 109. doi:10.1029/2002JB002251.

Clement, B.M., Connor, C.B., Graper, G., 1993. Paleomagnetic estimate of the emplacement temperature of the long-runout Nevado de Colima volcanic debris avalanche deposit, Mexico. Earth Planet. Sci. Lett. 120, 499–510.

Cogné, J.P., 2003. PaleoMac: a Macintosh™ application for treating paleomagnetic data and making plate reconstructions. Geochem. Geophys. Geosyst. 4 (1), 1007. doi:10.1029/2001GC000227.

Dermici, A., Görgülü, K., Durutürk, Y.S., 2004. Thermal conductivity of rocks and its variation with uniaxial and triaxial stress. Int. J. Rock Mech. Min. Sci. 41, 1133–1138.

Dobran, F., Papale, P., 1993. Magma–water interaction in closed systems and application to lava tunnels and volcanic conduits. J. Geophys. Res. 98, 14,041–14,058.

Downey, W.S., Tarling, D.H., 1991. Reworking characteristics of Quaternary pyroclastics, Thera (Greece), determined using magnetic properties. J. Volcanol. Geotherm. Res. 46, 143–155.

Druitt, T.H., 1998. Pyroclastic density currents. In: Gilbert, J.S., Sparks, R.S.J. (Eds.), The Physics of Explosive Volcanic Eruptions. . Geological Society, vol. 145. Special Publications, London, pp. 145–182.

Espíndola, J.M., Macías, J.L., Tilling, R.I., Sheridan, M.F., 2000. Volcanic history of El Chichón Volcano (Chiapas, Mexico) during the Holocene, and its impact on human activity. Bull. Volcanol. 62, 90–104.

Freundt, A., Bursik, M.I., 1998. Pyroclastic flow transport mechanisms. In: Freundt, A., Rosi, M. (Eds.), From Magma to Tephra, Modelling Physical Processes of Explosive Volcanic Eruptions. Elsevier, Amsterdam, pp. 173–231.

Gurioli, L., Pareschi, M.T., Zanella, E., Lanza, R., Deluca, E., Bisson, M., 2005. Interactions of pyroclastic density currents with human settlements: evidence from ancient Pompeii. Geology 33, 441–444. doi:10.1130/G21294.1.

Hoblitt, R.P., Kellogg, K.S., 1979. Emplacement temperatures of unsorted and unstratified deposits of volcanic rock debris by paleomagnetic techniques. Geol. Soc. Am. Bull. 90, 633–642.

James, D.W., 1968. The thermal diffusivity of ice and water between −40 and +60 °C. J. Mat. Sci. 540–543.

Jiménez, Z., Espíndola, V.H., Espíndola, J.M., 1999. Evolution of the seismic activity from the 1982 eruption of El Chichón volcano, Chiapas, Mexico. Bull. Volcanol. 61, 411–422.

Kent, D.V., Ninkovich, D., Pescatore, T., Sparks, R.S.J., 1981. Palaeomagnetic determination of emplacement temperature of Vesuvius AD 79 pyroclastic deposits. Nature 290, 393–396.

Kirschvink, J.L., 1980. The least-squares line and plane and the analysis of palaeomagnetic data. Geophys. J. R. Astron. Soc. 62, 699–718.

Kozu, S., 1934. The great activity of Komagatake in 1929. Mineral. Petrogr. Mitt. 45, 133–174.

Lipman, P.W., Mullineaux, D.R. (Eds.), 1981. The 1980 Eruptions of Mount St Helens, Washington. USGS Professional Paper, vol. 1250. 844 pp.

Luhr, J.F., Carmichael, I.S.E., Varekamp, J.C., 1984. The 1982 eruptions of El Chichón Volcano, Chiapas, Mexico: mineralogy and petrology of the anhydrite-bearing pumices. J. Volcanol. Geotherm. Res 23, 69–108.

Luhr, J., 1990. Experimental phase relations of water-and-sulfur saturated arc magmas and the 1982 eruption of El Chichón volcano. J. Petrol 31, 1071–1114.

Macías, J.L., Sheridan, M.F., Espíndola, J.M., 1997. Reappraisal of the 1982 eruptions of El Chichon volcano, Chiapas, Mexico: new data from the proximal deposits. Bull. Volcanol 59 (6), 459–471.

Macías, J.L., Espíndola, J.M., Bursik, M.I., Sheridan, M.F., 1998. Development of lithic breccias in the 1982 pyroclastic flow deposits of El Chichon Volcano, Mexico. J J. Volcanol. Geotherm. Res 83, 173–196.

Macías, J.L., Arce, J.L., Mora, J.C., Espíndola, J.M., Saucedo, R., Manetti, P., 2003. The ~ 550 bp Plinian eruption of el Chichón volcano, Chiapas, Mexico: explosive volcanism linked to reheating of a magma chamber. J. Geophys. Res. 108 (B12), 2569.

Mandeville, C.W., Carey, S., Sigurdsson, H., King, J., 1994. Paleomagnetic evidence for high-temperature emplacement of the 1883 subaqueous pyroclastic flows from Krakatau Volcano, Indonesia. J. Geophys. Res. 99, 9487–9504.

Marti, J., Diez-Gil, J.L., Ortiz, R., 1991. Conduction model for the thermal influence of lithic clasts in mixtures of hot gases and ejecta. J. Geophys. Res. 96, 21879–21885.

McClelland, E.A., Druitt, T.H., 1989. Palaeomagnetic estimates of emplacement temperatures of pyroclastic deposits on Santorini, Greece. Bull. Volcanol. 51, 16–27.

McClelland, E., Wilson, C.J.N., Bardot, L., 2004. Palaeotemperature determinations for the 1.8 - ka Taupo ignimbrite, New Zealand, and implications for the emplacement history of a high-velocity pyroclastic flow. Bull. Volcanol. 66, 492–513.

Medina-Martínez, F., 1982. El Volcán Chichón: GEOS, Boletín de la Unión Geofísica Mexicana, vol. 2(4), p. 19.

Müllerried, F.K.G., 1933. El Chichón, único volcán en actividad descubierto en el estado de Chiapas. Memorias de la Sociedad Científica Antonio Alzate 54, 411–416.

Özkahraman, H.T., Selver, R., Işik, E.C., 2004. Determination of the thermal conductivity of rock from P-wave velocity. Int. J. Rock Mech. Min. Sci. 41, 703–708.

Ryan, M.P., Banks, N.G., Hoblitt, R.P., Blevins, J.Y.K., 1990. The in-situ transport properties and the thermal structure of Mount St. Helens eruptive units. In: Ryan, M.P. (Ed.), Magma transport and storage. John Wiley, Hoboken, N.Y., pp. 137–155.

Rye, R.O., Luhr, J.F., Wasserman, M.D., 1984. Sulfur and oxygen isotopic systematics of the 1982 eruptions of El Chichón Volcano, Chiapas, Mexico. J. Volcanol. Geotherm. Res. 23, 109–123.

Scolamacchia, T., Macias, J.L., 2005. Distribution and stratigraphy of deposits produced by diluted pyroclastic density currents of the 1982 eruption of El Chichon volcano, Chiapas, Mexico. Revista Mexicana de Ciencias Geologicas 22, 159–180.

Scolamacchia, T., Macías, J.L., Sheridan, M.F., Hughes, S., 2005. Morphology of ash aggregates from wet pyroclastic surges of the 1982 eruption of El Chichon volcano, Mexico. Bull. Volcanol. 68, 171–200.

SEAN, 1989. Global volcanism 1975–1985. In: McClelland, L., Simkin, T., Summers, M., Nielsen, E., Stein, T.C. (Eds.), Smithsonian Institution Seismic Event Alert Network (SEAN). El Chichón, México and Central America, pp. 467–475.

Sigurdsson, H., Carey, S.N., Espindola, J.M., 1984. The 1982 eruptions of El Chichon volcano, Mexico: stratigraphy of pyroclastic deposits. J. Volcanol. Geotherm. Res 23, 11–37.

Sigurdsson, H., Carey, S.N., Fisher, R.V., 1987. The 1982 eruptions of El Chichon volcano, Mexico (3): physical properties of pyroclastic surges. Bull. Volcanol. 49, 467–488.

Sulpizio, R., Mele, D., Dellino, P., La Volpe, L., 2007. Deposits and physical properties of pyroclastic density currents during complex Subplinian eruptions: the AD 472 (Pollena) eruption of Somma-Vesuvius, Italy. Sedimentology 54, 607–635. doi:10.1111/j.1365-3091.2006.00852.x.

Sulpizio, R., Dellino, P., 2008. Sedimentology, depositional mechanisms and pulsating behaviour of pyroclastic density currents. In: Gottsman, J., Marti, J. (Eds.), Calderas volcanism: analysis, modelling and response. Elsevier, Amsterdam. Developments in Volcanology 10, 57–96.

Velinov, T.S., Bransalov, K., Mihovski, M., 1993. A thermal diffusion study of the solid phase of porous samples. Meas. Sci. Technol. 4, 1266–1268.

Vosteen, H.D., Schellschmidt, R., 2003. Influence of temperature on thermal conductivity, thermal capacity and thermal diffusivity for different types of rock. Phys. Chem. Earth. 499–509.

Wright, J.V., 1978. Remanent magnetism of poorly sorted deposits from the Minoan eruption of Santorini. Bull. Volcanol. 41, 131–135.

Yokoyama, I., De la Cruz-Reyna, S., Espíndola, J.M., 1992. Energy partition in the 1982 eruption of El Chichón volcano, Chiapas, Mexico. J. Volcanol. Geotherm. Res 51, 1–21.

Zanella, E., Gurioli, L., Pareschi, M.T., Lanza, R., 2007. Influences of urban fabric on pyroclastic density currents at Pompeii (Italy): 2. Temperature of the deposits and hazard implications. J. Geophys. Res. 112. doi:10.1029/2006JB004775.

Zanella, E., Gurioli, L., Lanza, R., Sulpizio, R., Bontempi, M., in press. Deposition temperature of the AD 472 Pollena pyroclastic density current deposits, Somma-Vesuvius, Italy. Bull. Volcanol. doi: 10.1007/s00445-008-0199-9.